Brief Report

DOI: 10.5582/ddt.2023.01014

Histopathological analysis revealed that *Mycobacterium abscessus* proliferates in the fat bodies of silkworms

Yasuhiko Matsumoto[1,*], Hanako Fukano[2], Harutaka Katano[3], Yoshihiko Hoshino[2,*], Takashi Sugita[1]

[1] Department of Microbiology, Meiji Pharmaceutical University, Tokyo, Japan;
[2] Department of Mycobacteriology, Leprosy Research Center, National Institute of Infectious Diseases, Tokyo, Japan;
[3] Department of Pathology, National Institute of Infectious Diseases, 1-23-1 Toyama, Shinjuku, Tokyo, Japan.

SUMMARY *Mycobacterium abscessus* causes chronic skin infections, lung diseases, and systemic or disseminated infections. Although a silkworm infection model with *M. abscessus* has been established, pathological analysis of the infected silkworms has not been performed. In this study, we performed hematoxylin-eosin and Ziehl-Neelsen staining of silkworms infected with *M. abscessus*. Four days after infection with *M. abscessus*, *M. abscessus* accumulation was observed in the fat bodies of silkworms. The number of viable *M. abscessus* cells in the fat bodies of the infected silkworms increased over time. These results suggest that *M. abscessus* proliferates in the fat bodies of the infected silkworms.

Keywords *Mycobacterium abscessus*, silkworm, fat body, infection

1. Introduction

Mycobacterium abscessus, is a group of rapidly growing non-tuberculous mycobacteria, causes chronic skin infections, lung diseases, and systemic or disseminated infections in immunocompromised patients (*1-4*). *M. abscessus* infections are associate with a greater lung function loss compared with cystic fibrosis caused by typical airway pathogens (*5*). High levels of antibiotic resistance in *M. abscessus* contribute to poor outcomes by limiting the treatment options (*6*). Several mouse *M. abscessus* infection models have been used to evaluate the efficacy of antibacterial drugs (*7*,*8*). These mouse infection models require several weeks to assess the mortality of infected mice. Moreover, long-term infection experiments using mice are difficult to conduct owing to animal welfare issues. The 3Rs, replacement, refinement, and reduction, are important animal welfare principles for experiments using mammals (*9*). To overcome these problems, a silkworm infection model with *M. abscessus* was established (*10*,*11*).

Silkworms are invertebrate animals that are beneficial for use in experiments to reveal host-pathogen interactions and identify candidates for antimicrobial drugs (*12-16*). Fewer ethical issues are associated with the use of a large number of silkworms for experimentation than with mammals (*17*). By exploiting this advantage of silkworms for infectious disease research, silkworm infection models are used as initial screening systems to identify virulence-related genes in pathogenic microorganisms (*18-21*). A silkworm infection model was established to evaluate anti-mycobacterial compounds using a type strain (*10*). Moreover, the virulence of *M. abscessus* clinical isolates was quantitatively evaluated by calculating the median lethal dose (LD_{50}), which is the dose of a pathogen required to kill half of the animals in a group, in a silkworm *M. abscessus* infection model (*11*). However, histopathological analysis of silkworms infected with *M. abscessus* has not yet been performed.

In the present study, we observed the accumulation of *M. abscessus* in the fat bodies of infected silkworms using histopathological analysis. Moreover, the number of viable *M. abscessus* cells increased in the fat bodies of infected silkworms. These findings suggest that the growth of *M. abscessus* in the fat bodies of infected silkworms might be a reason for the death of silkworms.

2. Materials and Methods

2.1. Reagents

Middlebrook 7H9 broth, Middlebrook 7H10 agar, and Middlebrook OADC enrichment were purchased from Becton, Dickinson, and Company (Sparks, MD, USA). Middlebrook 7H9 broth and Middlebrook 7H10 agar were supplemented with 10% Middlebrook OADC Enrichment. Hematoxylin-eosin (HE) was purchased

from Merck (Darmstadt, Germany). Ethanol, xylene, Ziehl carbol-fuchsine solution, and Loeffler's methylene blue solution were purchased from Muto Pure Chemicals Co. LTD (Tokyo, Japan).

2.2. Bacterial strain and culture condition

The *M. abscessus* subsp. *abscessus* ATCC19977 strain was used in this study. The *M. abscessus* ATCC19977 strain was grown on a Middlebrook 7H10 agar plate at 37°C. A single colony was then inoculated into 5 ml of Middlebrook 7H9 broth and incubated at 37°C for 3 days.

2.3. Infection experiments using silkworms

Silkworm infection experiments with *M. abscessus* were performed as previously described (*11*). Fifth-instar larvae were reared on an artificial diet (Silkmate 2S, Ehime-Sanshu Co., Ltd., Ehime, Japan) for 24 h. *M. abscessus* cells grown in Middlebrook 7H9 broth were collected by centrifugation and suspended in sterile saline. A 50-μL sample solution was administered to the silkworm hemolymph by injecting the silkworm dorsally using a 1-ml tuberculin syringe (Terumo Medical Corporation, Tokyo, Japan). Silkworms were injected with *M. abscessus* cells (1.4×10^7 cells per larva), and were incubated at 37°C for 4 days.

2.4. Histopathological analysis

Silkworms infected with *M. abscessus* were placed in 4% formalin and incubated at room temperature for two weeks (Figure 1). Paraffin-embedded sections of formalin-fixed silkworms were prepared and placed on glass slides.

HE staining was performed according to the manufacturer instruction. After immersion in xylene for 10 min, the specimens were immersed twice in 100% ethanol, and then in 95% ethanol, 80% ethanol, and 70% ethanol. After rinsing with water, specimens were immersed in Carracci's hematoxylin solution for 5 min. The specimens were immersed in 70% ethanol containing 0.2% hydrochloric acid, rinsed with water, and soaked in warm water for 10 min. After immersion in an alcohol eosin staining solution for 3 min, the specimens were quickly passed through 100% ethanol. The specimens were immersed in xylene for 3 min and sealed.

Ziehl-Neelsen staining was also performed according to the manufacturer instruction. Silkworm sections on glass slides were deparaffinized, removed xylene, and rinsed with distilled water. After immersion in Ziehl carbol-fuchsine solution for 30 min, the sections were rinsed under running water. After immersion in ethanol containing 0.5% hydrochloric acid for 10 seconds, sections were rinsed under running water. After 2 seconds of immersion in Loeffler's methylene blue solution, sections were lightly rinsed with water. The sections were dehydrated in 100% ethanol, immersed in xylene for 3 min, and sealed. Silkworm sections were examined under an optical microscope (BX51; Olympus, Tokyo, Japan).

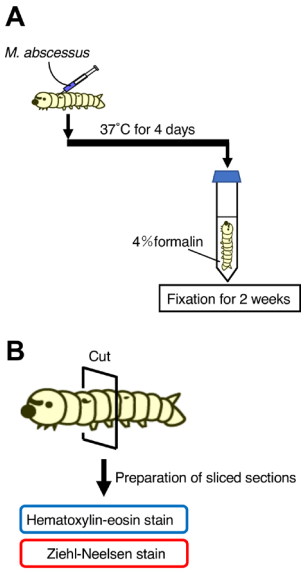

Figure 1. The experimental scheme of histopathological analysis of the silkworm infected with *M. abscessus* in this study. (**A**) Fixation of silkworms infected with *M. abscessus*. Silkworms were injected with saline or *M. abscessus* cells (1.4×10^7 cells per larva) and incubated at 37°C for 4 days. (**B**) Locations of sliced sections of silkworms.

2.5. Viable cell counts of *M. abscessus* in the silkworm fat body

Fat body isolation was performed as previously described (*22*). The silkworms were placed on ice for 15 min. Fat bodies were isolated from the dorsolateral region of each silkworm and rinsed with saline. The wet weights of the fat bodies were measured. The viable cell number of *M. abscessus* in the fat body of silkworms was measured according to a previous report (*23*). Silkworms were injected with *M. abscessus* cell suspension (7×10^6 cells in 50 μL) and incubated at 37°C. Fat bodies were harvested from silkworm larvae at 1, 2, 3, or 4 days post-infection. The fat body was homogenized in 1 mL of saline and the lysate was obtained. The lysate was 10^2 or 10^3-diluted with saline, and a 100 μL aliquot was spread on a Middlebrook 7H10 agar plate. The agar plate was incubated at 37°C for three days, and the colonies on the agar plates were counted. The viable cell number of *M. abscessus* per wet weight of fat body was determined.

2.6. Statistical analysis

The statistical significance of differences between viable cell counts of *M. abscessus* in silkworm groups was determined using Tukey's test. Statistical significance was set at $p < 0.05$.

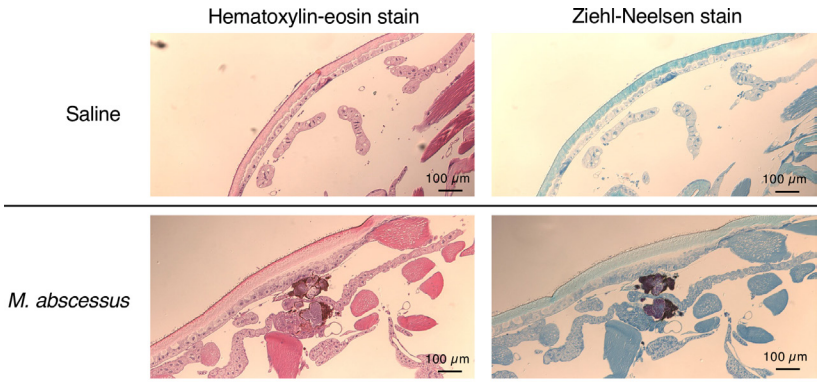

Figure 2. Histopathological analysis of sections from silkworms infected with or without *M. abscessus*. Silkworms were injected with saline or *M. abscessus* cells (1.4×10^7 cells per larva) and incubated at 37°C for 4 days. Silkworm sections were subjected to hematoxylin-eosin or Ziehl-Neelsen staining and observed under a microscope.

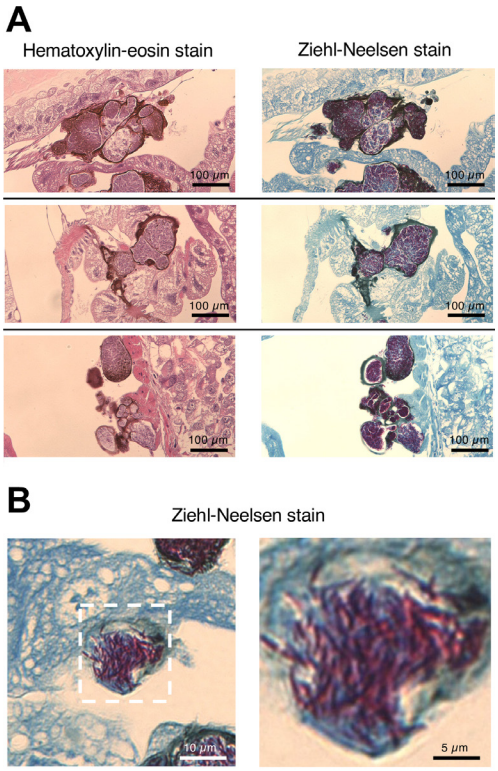

Figure 3. Accumulation of *M. abscessus* in the fat bodies of infected silkworm. (**A**, **B**) Silkworms were injected with *M. abscessus* cells (1.4×10^7 cells per larva) and incubated at 37°C for 4 days. Silkworm sections were subjected hematoxylin-eosin staining or Ziehl-Neelsen staining and observed under a microscope. (**A**) Three views of the fat bodies of the infected silkworm. (**B**) Red bacilli are observed.

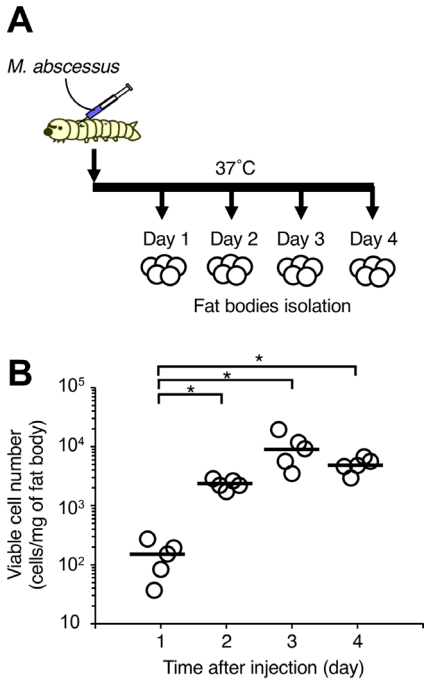

Figure 4. Increase in viable *M. abscessus* cells in the fat bodies of infected silkworms. (**A**) Experimental scheme. (**B**) Silkworms were injected with *M. abscessus* cells (7×10^6 cells in 50 μL) and were incubated at 37°C for 4 days. Silkworm fat bodies were isolated for four days after the injection of *M. abscessus*, and viable *M. abscessus* cells were counted. Five silkworms were used per group. The statistical significance of differences between viable cell counts of *M. abscessus* in silkworm groups was determined using Tukey's test. *: $p < 0.05$.

3. Results and Discussion

We performed histopathological analysis of the silkworms four days after infection with *M. abscessus*. *M. abscessus* cells (1.4×10^7 cells) were injected into silkworms, reared at 37°C for 4 days, and then immersed in 4% formalin solution for 2 weeks (Figure 1A). Silkworms were sliced into rings and subjected to hematoxylin-eosin and Ziehl-Neelsen staining (Figure 1B). In hematoxylin-eosin staining, a reddish brown area was observed in the fat bodies of the silkworms infected with *M. abscessus*, but not in those of the silkworms injected with saline (Figure 2). In the Ziehl-Neelsen staining, the area was stained dark red (Figure 2). Several areas stained dark red by Ziehl-Neelsen staining were observed in the fat bodies of silkworms infected with *M. abscessus* (Figure 3A). Red bacilli were observed in the fat bodies of silkworms infected with *M. abscessus* by Ziehl-Neelsen staining (Figure 3B). These results suggest that *M. abscessus* accumulates in the fat bodies of the silkworms.

Next, we examined whether *M. abscessus* grows in the fat bodies of the silkworms. The fat bodies of the silkworms were removed at 1, 2, 3, and 4 days after inoculation of silkworms with *M. abscessus*, and the number of viable *M. abscessus* cells in the fat bodies was determined (Figure 4A). The number of viable *M. abscessus* in the fat bodies of silkworms at 2, 3, and 4

days after inoculation with *M. abscessus* was higher than that at 1 day (Figure 4B). These results suggest that the fat body of the silkworm is the target of *M. abscessus* during infection.

In this study, *M. abscessus* accumulation was observed in the fat bodies of the silkworms. These foci differ from those of caseation necrosis, which are formed from aggregates of dead cells. A biofilm of *M. abscessus* complex in the pathologically thickened alveolar wall of the explanted lung of a patient with cystic fibrosis was observed (*24*). The foci of *M. abscessus* accumulation found in the infected silkworms were similar to those found in the lungs of a patient with cystic fibrosis. The establishment of a silkworm model of caseation necrosis caused by *M. abscessus* will be an important subject for future research.

In conclusion, we performed histopathological analysis of silkworms infected with *M. abscessus* and observed the accumulation of *M. abscessus* in their fat bodies. Furthermore, the number of viable *M. abscessus* cells in the fat bodies of silkworms infected with *M. abscessus* increased. These results suggest that *M. abscessus* grows in the fat bodies of the silkworms.

Acknowledgements

We thank Sachi Koganesawa, Hiromi Kanai, Yu Sugiyama, and Eri Sato (Meiji Pharmaceutical University) for their technical assistance rearing the silkworms. We also thank Maki Okuda, Sayaka Kashiwagi, and Ginko Kaneda for their assistance.

Funding: This study was supported in part by grants from the Japan Agency for Medical Research and Development/Japan International Cooperation Agency (AMED) to Y.H. (JP20fk0108064, JP20fk0108075, JP21fk0108093, JP21fk0108129, JP21fk0108608, JP21jm0510004, JP21wm0125007, JP21wm0225004, JP21wm0325003, JP22gm1610003, JP22wm0225022, JP22wm0325054), to H.F. (JP22wm0325054), and Y.M. (JP22wm0325054); and for Scientific Research (C) to Y.M. (JP20K07022) from the Japan Society for the Promotion of Science (JSPS).

Conflict of Interest: The authors have no conflicts of interest to disclose.

References

1. Catherinot E, Clarissou J, Etienne G, Ripoll F, Emile J-F, Daffé M, Perronne C, Soudais C, Gaillard J-L, Rottman M. Hypervirulence of a rough variant of the *Mycobacterium abscessus* type strain. Infect Immun. 2007; 75:1055-1058.
2. Esther CR, Esserman DA, Gilligan P, Kerr A, Noone PG. Chronic *Mycobacterium abscessus* infection and lung function decline in cystic fibrosis. J Cyst Fibros. 2010; 9:117-123.
3. Piersimoni C, Scarparo C. Pulmonary infections associated with non-tuberculous mycobacteria in immunocompetent patients. Lancet Infect Dis. 2008; 8:323-334.
4. Johansen MD, Herrmann JL, Kremer L. Non-tuberculous mycobacteria and the rise of *Mycobacterium abscessus*. Nat Rev Microbiol. 2020; 18:392-407.
5. Qvist T, Gilljam M, Jönsson B, *et al*. Epidemiology of nontuberculous mycobacteria among patients with cystic fibrosis in Scandinavia. J Cyst Fibros. 2015; 14:46-52.
6. Daley CL, Iaccarino JM, Lange C, *et al*. Treatment of Nontuberculous Mycobacterial Pulmonary Disease: An Official ATS/ERS/ESCMID/IDSA Clinical Practice Guideline. Vol. 71, Clinical infectious diseases: an official publication of the Infectious Diseases Society of America. 2020; pp. 905-913.
7. Obregón-Henao A, Arnett KA, Henao-Tamayo M, Massoudi L, Creissen E, Andries K, Lenaerts AJ, Ordway DJ. Susceptibility of *Mycobacterium abscessus* to antimycobacterial drugs in preclinical models. Antimicrob Agents Chemother. 2015; 59:6904-6912.
8. Maggioncalda EC, Story-Roller E, Mylius J, Illei P, Basaraba RJ, Lamichhane G. A mouse model of pulmonary *Mycobacteroides abscessus* infection. Sci Rep. 2020; 10:3690-3698.
9. Herrmann K, Pistollato F, Stephens ML. Beyond the 3Rs: Expanding the use of human-relevant replacement methods in biomedical research. ALTEX. 2019; 36:343-352.
10. Hosoda K, Koyama N, Hamamoto H, Yagi A, Uchida R, Kanamoto A, Tomoda H. Evaluation of anti-mycobacterial compounds in a silkworm infection model with *Mycobacteroides abscessus*. Molecules. 2020; 25:4971.
11. Matsumoto Y, Fukano H, Hasegawa N, Hoshino Y, Sugita T. Quantitative evaluation of *Mycobacterium abscessus* clinical isolate virulence using a silkworm infection model. PLoS One. 2022; 17:e0278773.
12. Hamamoto H, Urai M, Ishii K, *et al*. Lysocin E is a new antibiotic that targets menaquinone in the bacterial membrane. Nat Chem Biol. 2015; 11:127-133.
13. Nakamura I, Kanasaki R, Yoshikawa K, Furukawa S, Fujie A, Hamamoto H, Sekimizu K. Discovery of a new antifungal agent ASP2397 using a silkworm model of *Aspergillus fumigatus* infection. J Antibiot. 2017; 70:41-44.
14. Kaito C, Murakami K, Imai L, Furuta K. Animal infection models using non-mammals. Microbiol Immunol. 2020; 64:585-592.
15. Matsumoto Y. Facilitating drug discovery in human disease models using insects. Biol Pharm Bull. 2020; 43:216-220.
16. Montali A, Berini F, Brivio MF, Mastore M, Saviane A, Cappellozza S, Marinelli F, Tettamanti G. A silkworm infection model for *in vivo* study of glycopeptide antibiotics. Antibiotics (Basel). 2020; 9:300.
17. Matsumoto Y, Sekimizu K. Silkworm as an experimental animal to research for fungal infections. Microbiol Immunol. 2019; 63:41-50.
18. Kaito C, Kurokawa K, Matsumoto Y, Terao Y, Kawabata S, Hamada S, Sekimizu K. Silkworm pathogenic bacteria infection model for identification of novel virulence genes. Mol Microbiol. 2005; 56:934-944.
19. Hanaoka N, Takano Y, Shibuya K, Fugo H, Uehara Y, Niimi M. Identification of the putative protein phosphatase gene PTC1 as a virulence-related gene using a silkworm model of *Candida albicans* infection. Eukaryotic Cell.

2008; 7:1640-1648.
20. Ueno K, Matsumoto Y, Uno J, Sasamoto K, Sekimizu K, Kinjo Y, Chibana H. Intestinal resident yeast *Candida glabrata* requires Cyb2p-mediated lactate assimilation to adapt in mouse intestine. PLoS One. 2011; 6:e24759.
21. Paudel A, Hamamoto H, Panthee S, Matsumoto Y, Sekimizu K. Large-scale screening and identification of novel pathogenic *Staphylococcus aureus* genes using a silkworm infection model. J Infect Dis. 2020; 221:1795-1804.
22. Matsumoto Y, Ishii M, Hayashi Y, Miyazaki S, Sugita T, Sumiya E, Sekimizu K. Diabetic silkworms for evaluation of therapeutically effective drugs against type II diabetes. Sci Rep. 2015; 5:10722.
23. Matsumoto Y, Tateyama Y, Sugita T. Evaluation of antibacterial drugs using silkworms infected by *Cutibacterium acnes*. Insects. 2021; 12:619.
24. Qvist T, Eickhardt S, Kragh KN, Andersen CB, Iversen M, Høiby N, Bjarnsholt T. Chronic pulmonary disease with *Mycobacterium abscessus* complex is a biofilm infection. Eur Respir J. 2015; 46:1823-1826.

Received March 8, 2023; Revised April 5, 2023; Accepted April 6, 2023.

**Address correspondence to:*
Yasuhiko Matsumoto, Department of Microbiology, Meiji Pharmaceutical University, 2-522-1, Noshio, Kiyose, Tokyo 204-8588, Japan.
E-mail: ymatsumoto@my-pharm.ac.jp

Yoshihiko Hoshino, Department of Mycobacteriology, Leprosy Research Center, National Institute of Infectious Diseases, Tokyo, 189-0002, Japan.
E-mail: yhoshino@niid.go.jp

Released online in J-STAGE as advance publication April 12, 2023.